Deuterium NMR Structure of Retinal in the Ground State of Rhodopsin †

ARTICLE *in* BIOCHEMISTRY · NOVEMBER 2004

Impact Factor: 3.02 · DOI: 10.1021/bi0491191 · Source: PubMed

Deuterium NMR Structure of Retinal in the Ground State of Rhodopsin†

Gilmar F. J. Salgado,‡ Andrey V. Struts,§ Katsunori Tanaka,|| Naoko Fujioka,||,⊥ Koji Nakanishi,|| and Michael F. Brown*,‡,§,#

Departments of Biochemistry and Molecular Biophysics, Chemistry, and Physics, University of Arizona, Tucson, Arizona 85721, and Department of Chemistry, Columbia University, New York, New York 10027

Received April 30, 2004; Revised Manuscript Received June 12, 2004

ABSTRACT: The conformation of retinal bound to the G protein-coupled receptor rhodopsin is intimately linked to its photochemistry, which initiates the visual process. Site-directed deuterium (^{2}H) NMR spectroscopy was used to investigate the structure of retinal within the binding pocket of bovine rhodopsin. Aligned recombinant membranes were studied containing rhodopsin that was regenerated with retinal ^{2}H-labeled at the C_5, C_9, or C_{13} methyl groups by total synthesis. Studies were conducted at temperatures below the gel to liquid-crystalline phase transition of the membrane lipid bilayer, where rotational and translational diffusion of rhodopsin is effectively quenched. The experimental tilt series of ^{2}H NMR spectra were fit to a theoretical line shape analysis [Nevzorov, A. A., Moltke, S., Heyn, M. P., and Brown, M. F. (1999) *J. Am. Chem. Soc. 121*, 7636−7643] giving the retinylidene bond orientations with respect to the membrane normal in the dark state. Moreover, the relative orientations of pairs of methyl groups were used to calculate effective torsional angles between different planes of unsaturation of the retinal chromophore. Our results are consistent with significant conformational distortion of retinal, and they have important implications for quantum mechanical calculations of its electronic spectral properties. In particular, we find that the β-ionone ring has a twisted 6-*s*-*cis* conformation, whereas the polyene chain is twisted 12-*s*-*trans*. The conformational strain of retinal as revealed by solid-state ^{2}H NMR is significant for explaining the quantum yields and mechanism of its ultrafast photoisomerization in visual pigments. This work provides a consensus view of the retinal conformation in rhodopsin as seen by X-ray diffraction, solid-state NMR spectroscopy, and quantum chemical calculations.

G protein-coupled receptors (GPCRs)[1] are involved in numerous cellular communication and signal transduction pathways, and rhodopsin is currently a prototype for this group of pharmaceutically important biomolecules (*1*). Over 50% of the drugs currently used by humans affect GPCRs, which besides rhodopsin include the β-adrenergic receptor (*2*) and the opioid receptor (*3*). In the case of rhodopsin the ligand is 11-*cis*-retinal, which functions as an inverse agonist. Absorption of a visible photon triggers femtosecond isomerization of retinal (*4*), giving the active signaling state followed by the perception of light (*5*, *6*). Current knowledge indicates that the retinal chromophore is highly distorted in the region of the C_{11}═C_{12} double bond as well as the β-ionone ring (*7*, *8*). On the basis of deuterium (^{2}H) NMR spectroscopy (*9*) it has a 6-*s*-*trans* conformation, opposite to the crystal structure of 11-*cis*-retinal (*10*). Yet previous solid-state ^{13}C NMR measurements (*11*, *12*) and regeneration experiments with locked retinoids (*13*) indicate a 6-*s*-*cis* conformation, as suggested by the X-ray structure of rhodopsin (*14*−*16*). The biological importance of the β-ionone ring conformation is that photoaffinity labeling studies (*17*) suggest it is released from the retinal binding pocket in association with helical movements (*6*) that lead to activation of the photoreceptor. Aspects of the above picture remain controversial at present (*18*), and clearly one issue is how ^{2}H solid-state NMR studies of retinal bound to rhodopsin correspond to the results of other biophysical approaches.

We have been conducting studies of deuterated retinal bound to rhodopsin in aligned lipid bilayers, with the goal of developing ^{2}H NMR methods for investigations of membrane proteins (*19*). In ^{2}H solid-state NMR spectroscopy of oriented samples (*20*) the quadrupolar couplings provide angular restraints which allow one to investigate the conformation and orientation of various ligands bound to GPCRs. An earlier ^{2}H NMR structure of retinal bound to rhodopsin has been reported (*9*) but has been recanted on the basis of comparison to rotational resonance ^{13}C NMR

† This research was supported by grants from the National Institutes of Health (GM34509 to K.N. and EY12049 to M.F.B.). G.F.J.S. is the recipient of a predoctoral fellowship from the Institute for Biomedical Research and Biotechnology of the University of Arizona. K.T. is the recipient of a Japan Society for the Promotion of Science postdoctoral fellowship.

* To whom correspondence should be addressed at Department of Chemistry, University of Arizona. Tel: 520-621-2163. Fax: 520-621-8407. E-mail: mfbrown@u.arizona.edu.

‡ Department of Biochemistry and Molecular Biophysics, University of Arizona.

§ Department of Chemistry, University of Arizona.

|| Columbia University.

⊥ Current address: Shionogi & Co., Ltd., Osaka, Japan.

Department of Physics, University of Arizona.

[1] Abbreviations: DTAB, dodecyltrimethylammonium bromide; DMPC, 1,2-dimyristoyl-*sn*-glycero-3-phosphocholine; DTT, 1,4-dithiothreitol; EDTA, ethylenediaminetetraacetic acid; fwhm, full width at half-maximum; GPCR, G protein-coupled receptor; POPC, 1-palmitoyl-2-oleoyl-*sn*-glycero-3-phosphocholine; RMSD, root mean square deviation; MNDO, modified neglect of diatomic overlap; TD, transition dipole.

10.1021/bi0491191 CCC: $27.50
Published on Web 09/18/2004

distance measurements (*12*). Other ^{13}C solid-state NMR studies have investigated the structure of retinal within the binding pocket of rhodopsin (*18*, *21*, *22*), and solid-state ^{13}C NMR correlation spectroscopy has been used to determine the conformation of neurotensin bound to its GPCR (*23*). Here we present the three-dimensional structure of retinal within the binding pocket of rhodopsin based on ^2H solid-state NMR spectroscopy. We show that conformational strain of retinal when bound to bovine rhodopsin leads to a twisted 6-*s*-*cis* conformation of the β-ionone ring, whereas the polyene chain is twisted 12-*s*-*trans*. The conformational strain of retinal as seen by ^2H NMR has an important bearing on quantum mechanical calculations of retinal properties (*24*, *25*). Moreover, it is relevant to interpreting the ultrafast reaction dynamics of the 11-*cis* to *trans* photoisomerization of retinal within the rhodopsin binding pocket (*4*). Knowledge of the molecular basis of triggering of the visual signal is provided in relation to mechanisms of activation occurring within the GPCR superfamily.

EXPERIMENTAL PROCEDURES

Synthesis of Specifically Deuterated 11-cis-Retinals. Isotopically labeled retinals with deuterated C_5, C_9, or C_{13} methyl groups were synthesized using methods described elsewhere (*26*). They were characterized by their UV−visible spectra, Fourier transform infrared spectra, and their ^1H, ^2H, and ^{13}C NMR spectra. The deuterium content was established by ^2H NMR spectroscopy, which gave a single peak in benzene solution. Mass spectrometry in acetone/acetonitrile using positive electrospray ionization (ESI) further confirmed the purity of the synthetic deuterated retinals. The (quasi)-molecular MH^+ ions were at $m/z = 288.1$, consistent with a single deuterated methyl group, as compared with authentic 11-*cis*-retinal with MH^+ at $m/z = 285.1$.

Regeneration of Rhodopsin and Recombination with Synthetic Phospholipids. Rod outer segment membranes in HEPES buffer, pH 6.8, were isolated from frozen bovine retinas (W. L. Lawson Co., Lincoln, NE) as described (*27*). The rod membranes were bleached at 4 °C by exposure to yellow light ($\lambda > 520$ nm) for 30 min in the presence of 100 mM hydroxylamine (pH 6.8). The membrane suspension was then centrifuged and the pellet resuspended in hydroxylamine-free buffer, repeating this procedure at least four times. Synthetic deuterated 11-*cis*-retinal in EtOH was added in a 1.5 molar excess, and regeneration was carried out for 1.5 h at 37 °C. The regenerated rhodopsin was solubilized in dodecylammonium bromide (DTAB) and purified by hydroxyapatite chromatography, followed by recombination with 1-palmitoyl-2-oleoyl-*sn*-glycero-3-phosphocholine (POPC) (Avanti Polar Lipids, Alabaster, AL) at a 1:50 molar ratio by detergent dialysis (*27*). The recombinant rhodopsin/POPC samples contained 5 mM HEPES buffer, pH 6.8, prepared from ^2H-depleted ^1H_2O, and included 1 mM DTT and 1 mM EDTA. All final samples used for ^2H NMR had A_{280}/A_{500} ratios in the range of 1.6−2.2.

Preparation of Aligned Membrane Samples. Rhodopsin/POPC recombinant membranes (1:50 molar ratio) were oriented on ultrathin glass plates (Marienfeld Glassware, Bad Mergentheim, Germany) by isopotential ultracentrifugation (*28*). The aligned samples typically contained 22−25 mg of rhodopsin deposited on a total of 25 ultrathin glass plates. Membrane films were hydrated by isopiestic transfer in a sealed chamber containing saturated NaBr in ^2H-depleted ^1H_2O (relative humidity ≈63% at 4 °C), which was found to improve the alignment. Extensive ^{31}P NMR studies using a home-built, single-tuned ^{31}P NMR probe indicated that typically ≈90% of the sample was oriented by the procedure, the remaining unoriented fraction giving an underlying powder pattern (results not shown). The alignment disorder (mosaic spread) of the oriented fraction of the sample was obtained from ^2H NMR spectroscopy as described below. Tilt angles of the membrane stack relative to the static magnetic field were measured with a protractor and were estimated to be accurate to within ±2°.

Solid-State Deuterium NMR Spectroscopy. A modified Bruker AMX-500 spectrometer (11.7 T) was used in conjunction with a high-power radio frequency boost amplifier (Model Tempo 2006; Henry Radio, Los Angles, CA). Aligned membrane specimens were contained within the 8-mm horizontal solenoid radio frequency coil of a home-built high-power ^2H NMR probe, which gave a 4.2 μs 90° pulse at 76.77 MHz (rotating field strength of 59.5 kHz). Both a conventional quadrupolar echo pulse sequence ($90°_x-\tau-90°_y-\tau-$acquire) and a quadrupolar echo sequence with composite pulses ($135°_{-x}90°_x45°_{-x}-\tau-135°_y90°_{-y}45°_y-\tau-$acquire) (*29*) were employed and appropriately phase cycled to obtain the ^2H NMR signals. Control studies of deuterated polymethylmethylacrylate (PMMA-d_8) were routinely conducted and confirmed that high-fidelity ^2H NMR line shapes were obtained using both pulse sequences. The delay time τ ranged from 40 to 70 μs, depending on the sample temperature, to avoid acoustical ringing of the radio frequency coil, and the repetition time was typically 100−500 ms. The quadrupolar echo signals were apodized by exponential multiplication, corresponding to a 0.5 kHz line broadening. Fourier transformation was carried out using data processing software written in-house (MATLAB; The MathWorks, Inc., Natick, MA) and was initiated at the top of the quadrupolar echo, utilizing both quadrature data channels (no symmetrization which can lead to spectral artifacts). No first-order phase correction was applied to any of the spectra to eliminate the possibility of spectral distortions due to frequency-dependent phase shifts. The ^2H NMR spectra required a minimum of 300 000 scans at −150 °C up to $(1-3) \times 10^6$ scans at −60 °C (≈1−6 d of signal averaging for each spectrum).

RESULTS

Site-Specific Deuterium NMR Spectroscopy of Retinal within the Binding Pocket of Rhodopsin. In this work we have applied a site-directed, solid-state ^2H NMR approach for investigating ligands bound to GPCRs and other integral membrane proteins (*20*). Bovine rhodopsin ($M_r \approx 40$ kDa) was regenerated with synthetic 11-*cis*-retinal (*26*) that was selectively deuterated at the C_5, C_9, or C_{13} methyl positions. [The numbering of the methyl groups of retinal (*19*) follows organic nomenclature, where the correspondence to the crystallographic numbering of the carbon atoms (*10*) is C_5 methyl carbon ≡ C_{18}, C_9 methyl carbon ≡ C_{19}, and C_{13} methyl carbon ≡ C_{20} (*9*).] Rhodopsin containing deuterated 11-*cis*-retinal was then recombined with 1-palmitoyl-2-oleoyl-*sn*-glycero-3-phosphocholine (POPC) by detergent dialysis (1:50 molar ratio), and the membranes were aligned

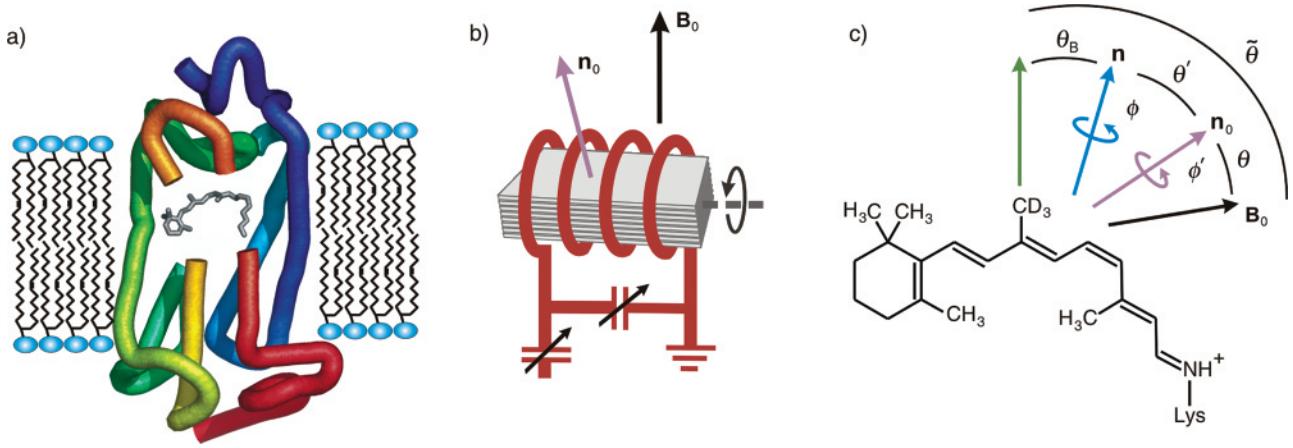

FIGURE 1: Experimental geometry for ^{2}H NMR line shape investigations of the 11-*cis*-retinal chromophore of rhodopsin. (a) Organization of rhodopsin within the membrane showing the retinal ligand within the binding pocket of the photoreceptor. (b) Schematic depiction of recombinant membranes containing rhodopsin aligned on ultrathin glass plates within the radio frequency coil of the NMR probe. The average normal to the membrane stack is designated by $\mathbf{n}_0$, and the direction of the main magnetic field is $\mathbf{B}_0$. (c) Illustration of relevant angles used for analytical line shape calculation of ^{2}H NMR spectra of a static uniaxial aligned sample (cf. text).

by isopotential centrifugation onto planar substrates (*28*). At temperatures below the gel to liquid-crystalline phase transition temperature of POPC (−4 °C), both the lipids and rhodopsin have static rotational disorder within the membrane plane. As a consequence, the recombinant samples comprised a static uniaxial distribution of the lipid and protein moieties on the NMR time scale (*19*) at all of the temperatures considered in this research.

The experimental studies involved recording tilt sequences of ^{2}H NMR spectra relative to the static magnetic field (*19*) for the aligned membranes containing rhodopsin labeled with ^{2}H at the various retinylidene methyl groups. We implemented a new theoretical ^{2}H NMR line shape treatment for a static uniaxial distribution (*20*) to deduce local angular constraints for the retinylidene prosthetic group of rhodopsin. In the present application, the ^{2}H NMR spectrum depends on the angle $\tilde{\theta}$ between an individual C−C^{2}H$_3$ bond axis of the retinal molecule and the direction of the main magnetic field (*30*). The line shape for such an aligned sample is described by a semirandom distribution of the C−C^{2}H$_3$ bond axes within the angular space of the membrane, which in turn is mapped into the frequency space of the ^{2}H NMR spectrum. A schematic illustration is given in Figure 1, part a, which depicts the folding of the rhodopsin polypeptide chain within the membrane, together with the bound retinal ligand. In part b of Figure 1, the stack of ≈25 ultrathin glass slides containing the aligned recombinant membranes is shown inserted into the radio frequency coil of the NMR probe. The average normal to the membrane stack is designated by $\mathbf{n}_0$, and the main magnetic field is indicated by $\mathbf{B}_0$. Lastly, the ^{2}H-labeled 11-*cis*-retinal is illustrated in Figure 1, part c, where the overall orientation $\tilde{\theta}$ of the C−C^{2}H$_3$ bond axis relative to $\mathbf{B}_0$ is decomposed into various Euler angles using the closure property of the group of rotations (*30*).

Referring to Figure 1, part c, the parameters of the line shape simulations include the C−C^{2}H$_3$ orientation (θ_B) relative to the membrane normal $\mathbf{n}$, which provides the angular constraint on the retinal conformation, together with the alignment disorder (so-called mosaic spread) of the membrane stack. In part c, θ' represents the angle of the local normal $\mathbf{n}$ relative to the average membrane normal $\mathbf{n}_0$, which describes the (Gaussian) alignment disorder, and θ is the angle between the average normal $\mathbf{n}_0$ and the main magnetic field $\mathbf{B}_0$, which accounts for the tilt series of the ^{2}H NMR spectra. Note that two static axial distributions are involved in the line shape analysis; these are described by ϕ, the azimuthal angle about the *local* membrane normal $\mathbf{n}$, and ϕ', the azimuthal angle about the *average* normal $\mathbf{n}_0$ to the stack of aligned membranes. The ϕ rotation means that the rhodopsin molecules within the membrane are uniformly distributed about the local normal axis, whereas the ϕ' rotation implies that the various membranes are themselves uniformly distributed about the average alignment axis. If the second azimuthal rotation ϕ' is neglected in treating the mosaic spread (*31*), then this is equivalent to the disregard of longitude in geography, specifying the position of a point on the earth's surface only by its colatitude, θ' in our notation, which is incorrect. Indeed, for tilting of $\mathbf{n}_0$ away from the magnetic field direction such a treatment (*31*) fails to reproduce the appropriate powder pattern of a Pake doublet in the limit of infinite mosaic spread (*20*). Further description of the theoretical details of the solid-state ^{2}H NMR line shape simulations is provided below.

Turning next to Figure 2, we show representative experimental ^{2}H NMR spectra of rhodopsin/POPC recombinant membranes containing 11-*cis*-retinal deuterated at the C_5 methyl group of the β-ionone ring. Deuterium NMR spectra for aligned membranes were recorded at a temperature of −60 °C, well below the gel to liquid-crystalline phase transition of POPC. The ^{2}H NMR spectra are indicative of rapidly rotating methyl groups on the ^{2}H NMR time scale, as also verified by studies of unoriented powder-type samples (results not shown). In these experiments the average bilayer normal $\mathbf{n}_0$ was inclined at tilt angles of $\theta = 0°$ or 90° relative to the main magnetic field $\mathbf{B}_0$. Part a of Figure 2 presents the experimental ^{2}H NMR spectra superimposed with theoretical fits for a static uniaxial distribution (*20*). The value of the bond axis orientation is $\theta_B = 70 \pm 3°$ and the mosaic spread is $\sigma = 21 \pm 2°$, which were determined for the C_5 methyl group from simultaneous nonlinear regression fitting of the angular-dependent spectral data (vide infra). For the C_9 and C_{13} methyl groups of retinal, respectively, we obtained bond axis orientations of $\theta_B = 52 \pm 3°$ and $68 \pm 2°$ from

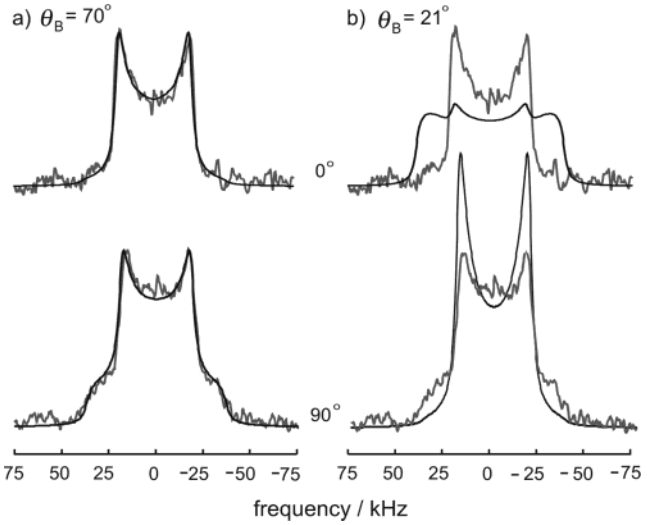

FIGURE 2: Comparison of solid-state ^{2}H NMR spectra of aligned membranes containing rhodopsin labeled with ^{2}H at the retinal C_5 methyl group at −60 °C to theoretical line shape simulations. Results are shown for the $\theta = 0°$ and 90° orientations of the normal to the membrane stack relative to the static magnetic field. Experimental ^{2}H NMR spectra are indicated in gray, and theoretical spectra obtained by simultaneously fitting the results for both bilayer orientations are depicted by solid dark lines. The experimental and simulated ^{2}H NMR spectra are normalized to constant area. (a) Angular-dependent ^{2}H NMR spectra and line shape simulations corresponding to a C−C^{2}H$_3$ bond orientation of $\theta_B = 70 \pm 3°$ and mosaic spread of $\sigma = 21 \pm 2°$, obtained by simultaneously fitting the data. (b) Line shape simulations of the same ^{2}H NMR spectra obtained by constraining $\theta_B = 21°$ as previously determined (*9*), together with the mosaic spread found in part a. The line shape simulations assume a (residual) quadrupolar coupling constant of $\langle\chi_Q\rangle = 39$ kHz and a Lorentzian full width at half-maximum (fwhm) = 4.0 kHz.

simultaneously fitting the ^{2}H NMR spectra at the two tilt orientations of $\theta = 0°$ and 90° (results not shown).

For comparison, part b of Figure 2 shows theoretical simulations of the same experimental ^{2}H NMR spectra assuming a C−C^{2}H$_3$ bond orientation of $\theta_B = 21°$, as reported earlier (*9*), together with the above value of the mosaic spread. Here the experimental line shapes for the C_5 methyl group are not well reproduced, and hence we conclude that the value of $\theta_B = 70 \pm 3°$ determined in this work represents the more accurate value. Moreover, we attempted to fit the angular-dependent ^{2}H NMR spectra by constraining the C_5 bond orientation θ_B at the previous value (*9*) and allowing the mosaic spread to vary. In this case, the goodness of fit improved continuously with increasing mosaic spread up to $\sigma = 90°$ (results not shown), corresponding to the limit of a Pake doublet for randomly oriented bilayers (*20*). However, this finding disagrees with ^{31}P NMR spectral data obtained for the same samples, which indicate that the degree of alignment is ≈90% (cf. Experimental Procedures). Similar conclusions apply to the C_9 and C_{13} methyl positions. Briefly, the discrepancy with earlier work (*9*) may originate from a lack of consideration of the full three-dimensional character of the mosaic spread of the aligned samples (*31*), symmetrization of the experimental ^{2}H NMR spectra which can lead to artifactual quadrupolar splittings (*32*), and the rather low signal to noise of the previous ^{2}H NMR spectra obtained for static aligned samples (*33*) or aligned samples using magic-angle oriented-sample spinning (MAOSS) (*9*).

One should also note that the present work has employed rhodopsin/POPC recombinant membranes mainly at a temperature of −150 °C, whereas previously reported ^{2}H NMR studies of rhodopsin/DMPC recombinants were conducted at −60 °C (*9*). In addition, earlier ^{13}C solid-state NMR studies used a hydrated gel of rhodopsin solubilized in the detergent Ammonyx LO at ≈−30 °C (*11*), and X-ray crystallography of rhodopsin is typically carried out at a temperature of ≈−170 °C (*16*). Although differences in sample conditions might account for variations in the results from individual laboratories, we view this as unlikely for the following reasons. First, the electronic spectral properties of retinal are sensitive to its conformation; an appreciable bathochromic shift of ≈20−25 nm is found on going from a 6-*s*-*cis* to a 6-*s*-*trans* conformation of the β-ionone ring (*34*, *35*). But for rhodopsin recombined with POPC or DMPC, as well as rhodopsin solubilized in nonionic detergents (Ammonyx LO) or cationic detergents (DTAB), the UV−visible absorption spectra are essentially unperturbed as compared to the native retinal rod membranes, with a wavelength maximum at 500 nm (*27*, *36*, *37*). The so-called opsin shift is the same for rhodopsin in the various lipid and detergent environments studied, and hence the β-ionone ring conformation is unaltered. Second, we have also obtained preliminary ^{2}H NMR spectra for the C_5, C_9, and C_{13} methyl groups of retinal bound to rhodopsin at −30 °C, which closely resemble those at −150 °C (results not shown). Thus we conclude that changes in the retinal conformation when bound to rhodopsin are minimal over the temperature range from −30 to −150 °C.

Solid-State NMR Spectral Line Shape Analysis for Integral Membrane Proteins Containing Bound Ligands. We next turn to the structural analysis of retinal within the binding pocket of rhodopsin in the dark-adapted state. Representative experimental ^{2}H NMR spectra acquired at −150 °C for the retinal C_9 methyl group of rhodopsin are plotted in Figure 3, part a, for bilayer orientations ranging from $\theta = 0°$ to $\theta = 90°$. Compared with earlier data (*33*), substantially different ^{2}H NMR spectra were recorded. Most notable are the significant changes in the ^{2}H NMR spectral line shape as a function of the tilt angle θ; similar results were obtained at −60 °C. At the smaller tilt angles ($\theta = 0°$, 15°), the ^{2}H NMR spectra are rounded or flat in the center, whereas at larger tilt angles ($\theta = 60°$, 90°) the two transitions of the $I = 1$ quadrupolar ^{2}H nucleus are clearly evident.

To further interpret the angular-dependent ^{2}H NMR line shapes, theoretical simulations are necessary. For the case of rhodopsin, we recall that the theoretical ^{2}H NMR analysis (cf. Figure 1) involves the C−C^{2}H$_3$ bond orientation θ_B relative to the local membrane frame, together with the static misalignment of the membrane stack σ (mosaic spread). Assuming a uniaxial static distribution, as in aligned membranes below their order−disorder phase transition temperature, the following result is obtained for the ^{2}H NMR line shape (*20*):

$$|p(\xi_\pm)| \propto \frac{1}{|\cos\tilde{\theta}|}\int_0^\pi F(x,y)\, e^{-\theta'^2/2\sigma^2} \sin\theta'\, d\theta' \qquad (1)$$

Here $p(\xi_\pm)$ is the distribution of the spectral intensity as a function of the reduced frequency $\xi_\pm$ for the two $I = 1$ spectral branches, as given by $\xi_\pm = \pm 1/2(3\cos^2\tilde{\theta} - 1)$.

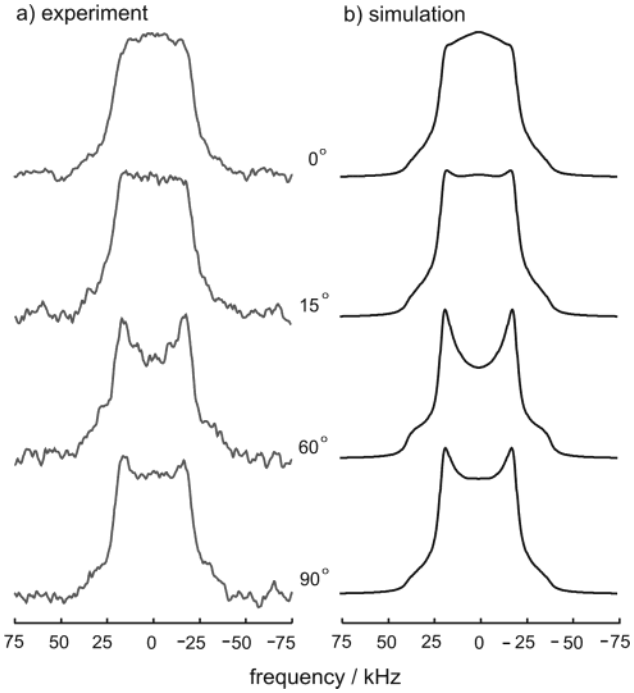

FIGURE 3: Representative solid-state ^{2}H NMR spectra obtained for rhodopsin/POPC (1:50 molar ratio) membranes labeled with ^{2}H at the retinal C_9 methyl group in the dark state. (a) Experimental ^{2}H NMR spectra acquired at −150 °C and (b) theoretical spectra calculated for a static uniaxial distribution of rhodopsin molecules. The orientation (tilt) of the normal to the membrane stack (θ) is indicated in the figure. The line shape simulation parameters are as follows: bond orientation $\theta_B = 52$ deg; mosaic spread $\sigma = 21°$; (residual) quadrupolar coupling constant $\langle\chi_Q\rangle = 39$ kHz; Lorentzian fwhm = 5.0 kHz. (The line widths of the simulated ^{2}H NMR spectra correspond to the convolution of the intrinsic line broadening of the sample and the window function used for processing the spectral data; cf. Experimental Procedures.)

Referring back to Figure 1, part c, the overall angle between the methyl bond axis and the magnetic field is $\tilde{\theta}$, and θ' is the inclination (tilt) of the local bilayer normal from its average value. The function $F(x,y)$ involves sums or differences of the above angles, together with θ_B, the methyl bond angle to the local membrane normal, and θ, the angle the average bilayer normal makes with the magnetic field. In eq 1 $x \equiv [(\gamma - \delta)(\alpha - \beta)]^{1/2}$ and $y \equiv [(\alpha - \delta)(\gamma - \beta)]^{1/2}$, where the cosines of the sum and difference angles are $\alpha \equiv \cos(\tilde{\theta} - \theta_B)$, $\beta \equiv \cos(\tilde{\theta} + \theta_B)$, $\gamma \equiv \cos(\theta - \theta')$, and $\delta \equiv \cos(\theta + \theta')$. The integrand is (i) $F(x,y) = y^{-1}\boldsymbol{K}(x/y)$ if $\alpha > \gamma > \delta > \beta$ or $\gamma > \alpha > \beta > \delta$ or (ii) $F(x,y) = x^{-1}\boldsymbol{K}(y/x)$ if $\gamma > \alpha > \delta > \beta$ or $\alpha > \gamma > \beta > \delta$. Here the kernel $\boldsymbol{K}(k) = F(\pi/2,k)$ represents a complete elliptic integral of the first kind in the normal trigonometric form (*20*). The mosaic spread is represented by a three-dimensional Gaussian distribution, where σ is the standard deviation about the mean of $\langle\theta'\rangle = 0$.

For the purpose of illustration Figure 3, part b, shows theoretical ^{2}H NMR spectra calculated for rhodopsin ^{2}H-labeled at the retinal C_9 methyl position using the above formalism. Closed-form simulations used the analytical line shape formula, eq 1, and included the C−C^{2}H$_3$ bond orientation, the mosaic spread, the residual quadrupolar coupling constant $\langle\chi_Q\rangle$ for the rotating methyl group, and the intrinsic spectral line width. The results of the theoretical simulations correspond well with the experimental ^{2}H NMR spectra in part a, showing the role of the C−C^{2}H$_3$ bond orientation and evincing the importance of a proper three-dimensional treatment of the alignment disorder (*20*). It is worth noting that the mosaic spread cannot simply be expressed as an extra contribution to the line broadening, but rather it contributes to the line shape in a more complex way (*20*). Moreover, for bond orientations greater than 35.3° there is typically an ambiguity in the sign of the quadrupolar (or dipolar) coupling. Therefore, if the ^{2}H solid-state NMR spectra are recorded only at zero tilt, e.g., as in the case of flat coils, then due to the sign ambiguity one obtains different calculated bond orientations (*19*). To distinguish these geometric solutions, it is necessary to obtain a rotation pattern (tilt series) of the ^{2}H NMR spectra as a function of the membrane tilt angle (*19*), as we describe below.

Global Fitting of Tilt Series of Solid-State Deuterium NMR Spectra of Retinylidene ^{2}H-Labeled Rhodopsin. By simulating the ^{2}H NMR spectra obtained for different membrane tilt angles, it is possible to determine the orientations of the C_9 and C_{13} methyl carbons of the retinal polyene chain and the C_5 methyl carbon of the β-ionone ring relative to the membrane normal. In Figure 4, the root mean square deviation (RMSD) of the calculated line shapes from the experimental ^{2}H NMR spectra for the C_5, C_9, and C_{13} positions is plotted against the C−C^{2}H$_3$ bond angle (θ_B) and the mosaic spread (σ), respectively. The error surfaces for the C_5 and C_{13} methyl positions are somewhat asymmetric, parts a and c, whereas that for the C_9 methyl group is relatively symmetric, part b. Nonetheless, Figure 4 indicates that well-defined minima are obtained in each case. From the global fits we obtained C−C^{2}H$_3$ bond angles of 70 ± 3°, 52 ± 3°, and 68 ± 2° for the C_5, C_9, and C_{13} methyl groups, respectively (Table 1), with σ in the range of 18−21°. One should note that the mosaic spread refers to the oriented fraction of the samples, which based on ^{31}P NMR studies is determined to be ≈90% (cf. Experimental Procedures).

On the other hand, the previously reported values (*9*) for the C_5, C_9, and C_{13} methyl bond orientations of $\theta_B = 21°$, 44°, and 30° give RMSD values that are substantially higher than those in Figure 4. Variation of the mosaic spread σ does not lead to well-defined minima, with the possible exception of the C_9 methyl group (results not shown). Although the methyl bond orientations obtained in the present work differ from those reported previously (*9*), they are in excellent agreement with the refined crystal coordinates of rhodopsin (*15*). Compared to the first (*14*) and third (*16*) crystal structures, the correspondence is not as good, though still satisfactory. One should also note that the values for the bond orientation θ_B and mosaic spread σ obtained from the global fit of the tilt series of ^{2}H NMR spectra (cf. Figure 4) correspond well with the results of fitting only the $\theta = 0°$ and 90° spectra (cf. Figure 2). This observation suggests that, for certain applications, acquiring ^{2}H NMR spectra at just the two bilayer orientations of $\theta = 0°$ and 90° may be sufficient.

Calculation of Effective Torsion Angles. In what follows, we shall assume the retinal conformation is essentially described by the orientations of the β-ionone ring and the planes of conjugation on either side of the 11-*cis* double bond (*8*). Figure 5 shows that the three planes, A, B, and C, have two shared bonds, and consequently there are four angular

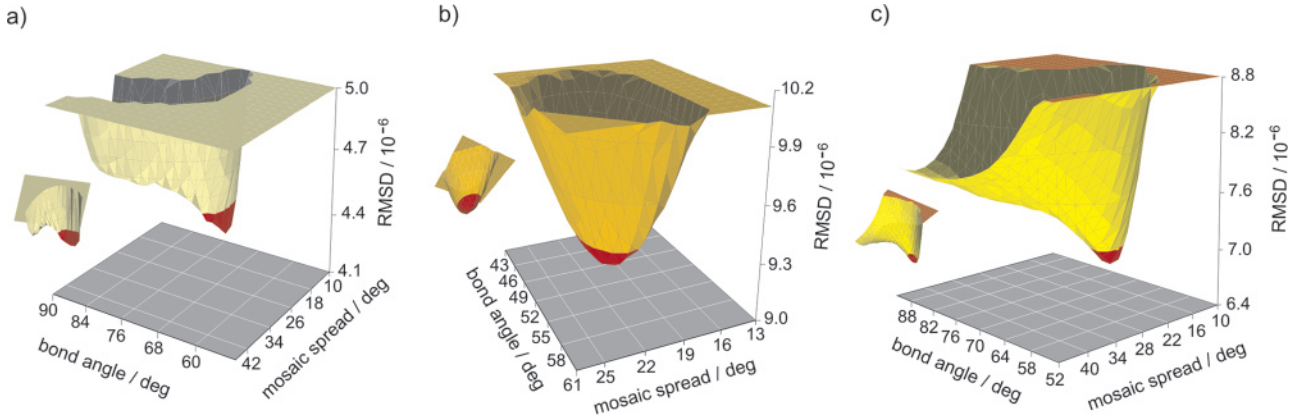

FIGURE 4: Global fitting of theoretical ^{2}H NMR line shapes for aligned rhodopsin/POPC membranes containing retinal ^{2}H-labeled at (a) C_5, (b) C_9, and (c) C_{13} methyl groups at −150 °C. The root mean square deviation (RMSD) of the calculated ^{2}H NMR spectral line shapes from the experimental tilt series (normalized) is shown as a function of the C−C^{2}H$_3$ bond angle (θ_B) and the mosaic spread (σ). A well-defined global minimum is obtained in each case, shown in red color, with the bond orientations summarized in Table 1. Values of the mosaic spread fall in the range of $\sigma = 18-21°$ for the C_5, C_9, and C_{13} methyl groups.

Table 1: Retinal Conformation in the Ground State of Rhodopsin

	bond orientation (θ_B/deg)			torsional angle/deg	
				C_5=C_6−C_7=C_8	C_{11}=C_{12}−C_{13}=C_{14}
structure	C_5	C_9	C_{13}		
crystal (1F88)[a,b]	73.6	65.2	54.6	−59	171
crystal (1HZX)[a,b]	70.9	53.9	69.5	−57	156
crystal (1L9H)[a,b]	67.8	56.2	58.6	−77	171
^{2}H NMR[c,d]	21 ± 5	44 ± 5	30 ± 5		
^{2}H NMR[d−f]	70 ± 3	52 ± 3	68 ± 2	−65	150

[a] Protein Data Bank (PDB) accession code. [b] Methyl bond orientations were calculated relative to the *z*-axis of the inertial tensor of rhodopsin, assumed to correspond to the bilayer normal. The principal axes of the inertial tensor were obtained by diagonalizing the values obtained from the atomic coordinates of the PDB file. [c] Reference *9*. [d] Bond orientations refer to the angle between the C−C^{2}H$_3$ axis and the normal to the local membrane surface. Due to the even parity of the quadrupolar interaction tensor in ^{2}H NMR, the bond orientation θ_B cannot be distinguished from its supplement $\pi-\theta_B$. [e] This work; errors correspond to the inverse curvature matrix of the χ^2 hypersurface utilized for the nonlinear regression fits. [f] Torsion angle calculations include additional constraints (cf. text).

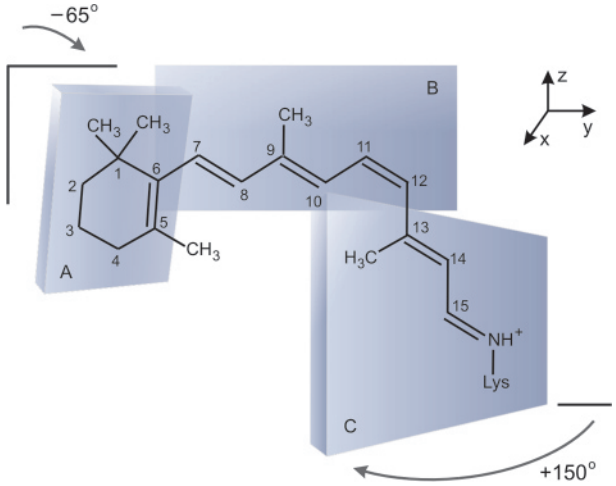

FIGURE 5: Calculated structure of retinal within the binding pocket of rhodopsin at −150 °C based on ^{2}H NMR angular restraints. The rotational degrees of freedom are approximated in terms of three planes, A, B, and C; i.e., additional twisting of the polyene chain is not considered. Planes B and C have a relative orientation specified by the torsional angle of the $C_{12}-C_{13}$ bond, which is +150°. The relative orientation of the A and B planes, i.e., the conformation of the β-ionone ring relative to the polyene chain, is due to the C_6-C_7 torsional angle with a value of −65°.

degrees of freedom. Three of these angles are determined by the C_5, C_9, and C_{13} methyl groups (Table 1); as a fourth parameter, we introduce the orientation of the electronic transition dipole moment from linear dichroism studies (*38*). All of our calculations assume ideal orbital hybridization, or they include deviations from the ideal bond angles as found in the crystal structure of 11-*cis*-retinal (*10*).

For a pair of methyl groups (i, k) attached to different planes of the retinal molecule, the effective torsion angle $\chi_{i,k}$ is given by

$$\chi_{i,k} = \cos^{-1}\left(\frac{\cos\theta_i \cos\theta_B{}^{i,k} - \cos\theta_B{}^{i}}{\sin\theta_i \sin\theta_B{}^{i,k}}\right) - \cos^{-1}\left(\frac{\cos\theta_k \cos\theta_B{}^{i,k} - \cos\theta_B{}^{k}}{\sin\theta_k \sin\theta_B{}^{i,k}}\right) \quad (2)$$

The derivation of eq 2 employs the closure property of the rotation group (*30*) and is relatively straightforward. In this expression $\theta_B{}^i$ and $\theta_B{}^k$ are the individual methyl bond orientations relative to the membrane normal (Table 1), and θ_i and θ_k designate their angles with respect to the bond whose torsion angle is $\chi_{i,k}$. (Here we introduce the additional labels i, k to designate specific methyl groups of the retinal molecule, which are suppressed in the preceding notation.) The angle of the bond axis joining two planes relative to the membrane normal is denoted as $\theta_B{}^{i,k}$ and is calculated either from the electronic transition dipole moment (*38*, *39*) or from the methyl group orientation in the case of ^{2}H NMR. Note that the sense (sign) of the torsion angle, corresponding to the chiral selectivity of the binding pocket, cannot be determined from eq 2 due to the even functions. Furthermore, the nuclear spin interactions in solid-state NMR have even parity (*40*), so that the various angles cannot be distinguished from their supplements. As a result we are unable to differentiate between twisted *s-cis* and *s-trans* conformations, contrary to an earlier report (*9*). Rather, 16 symmetry-related solutions are obtained for each of the effective torsion angles. Some of the solutions are degenerate, however, and by considering ^{13}C NMR rotational resonance (*12*, *41*), chemical

shift (*11*), and circular dichroism (*8*) data, most of these can be eliminated.

Conformational Analysis of Retinal within the Binding Pocket of Rhodopsin. The ^{2}H NMR data presented above have important implications with regard to the retinal conformation when bound to the dark state of rhodopsin. Here we show how the relative orientations of the ^{2}H nuclear spin coupling tensors of the different deuterated methyl groups of retinal allow one to estimate the torsional angles involving the various planes of unsaturation of the molecule. In this way, it is possible to investigate the three-dimensional structure of the retinal ligand within its protein binding pocket. As described in greater detail below, analysis of the data in Table 1 allows us to conclude that there are out-of-plane twists of the β-ionone ring (A) relative to the C_6-C_{13} plane of conjugation (B), as well as twists of the C_6-C_{13} plane relative to the $C_{12}-C_{15}$ plane (C). The twisting arises from conformational stress and strain of the retinal chromophore due to the induced fit to the rhodopsin binding pocket.

Now according to Figure 5, the torsion angle of the $C_{12}-C_{13}$ bond is defined by the orientation of the C_6-C_{13} plane of unsaturation (B) relative to the $C_{12}-C_{15}$ plane (C). The torsional twist about the $C_{12}-C_{13}$ bond manifests the chromophore distortion adjacent to the 11-*cis* double bond, where isomerization occurs due to photolysis. However, the C_9 axis is collinear with the $C_{12}-C_{13}$ bond, assuming ideal orbital geometry, and thus further information must be introduced. Consequently, we also make use of the orientation of the retinal transition dipole moment with respect to the bilayer normal, as obtained from linear dichroism data (*38*, *39*). Very briefly, applying eq 2 to the relative orientations of the transition dipole (TD) and the C_{13} methyl group yields the result that the polyene chain conformation is either twisted 12-*s*-*trans* or twisted 12-*s*-*cis*. Either ideal orbital geometry is adopted or the $C_{11}=C_{12}-C_{13}$ bond angle is assumed to be 130° as found in the crystal structure of 11-*cis*-retinal (*10*). In either case the $C_{12}-C_{13}$ bond tilt is obtained directly from the ^{2}H NMR result of 52° for the C_9 methyl group (Table 1). In this way, assuming values of $\theta_{TD} = \pm 74°$ ($\pm 64°$), $\theta_B^{TD} = 74°$, $\theta_{13} = \pm 60°$ ($\pm 60°$), and $\theta_B^{13} = 68°$, we obtain solutions for the effective torsion angle of $\chi_{9,13} = 0$ (∓ 8), ± 44 (± 53), (± 24), (± 73), ± 152 (± 150), and ± 164 (± 172)°, where the values assuming ideal orbital geometry are provided first, and those calculated using the crystal structure of 11-*cis*-retinal are given in parentheses. (Note that here the $\pm$ symbol refers to the sense of the dihedral angle rotation.)

The allowed solutions can be further restricted, e.g., by including distance constraints from rotational resonance ^{13}C NMR (*41*), as well as data for retinal derivatives (*8*). Comparing the distances between carbon atoms $C_{10}-C_{20}$ and $C_{11}-C_{20}$ calculated using the retinal geometry to those obtained from rotational resonance ^{13}C NMR studies (*41*), and assuming a positive twist for the torsional angle as indicated by studies of locked retinoids (*8*), leads to the unique physical solution of $\chi_{9,13} = +150°$ corresponding to a positively twisted, 12-*s*-*trans* conformation (Figure 5). This result is consistent with magic-angle spinning ^{13}C NMR measurements of the chemical shift tensors of retinylidene ^{13}C-labeled rhodopsin (*11*) and with regeneration studies and circular dichroism data for locked retinoids (*8*), which also indicate a 12-*s*-*trans* conformation. Assuming the C_6-C_{13} and $C_{12}-C_{15}$ regions of the polyene chain are nearly planar, the twist represents the effective torsional angle of the $C_{12}-C_{13}$ bond (*15*).

Likewise, the relative orientations of the pair of C_5 and C_9 methyl groups describe the twist of the β-ionone ring, i.e., the C_5-C_7 plane of unsaturation (A) relative to the C_6-C_{13} plane (B). For the case of the C_5 and C_9 pair of methyl groups, the C_6-C_7 bond tilt of 45° was calculated from the C_5 and C_9 data, where the other angles are $\theta_5 = \pm 60°$, $\theta_B^5 = 70°$, $\theta_9 = \pm 60°$, and $\theta_B^9 = 52°$. Applying eq 2, we obtain as possible solutions $\chi_{5,9} = \pm 5$, ± 24, ± 53, ± 65, ± 65, ± 111, ± 154, and ± 159°, where ideal hybrid orbitals are assumed similar to the X-ray structure of 11-*cis*-retinal (*10*). If the distance constraints from rotational resonance ^{13}C NMR studies (*12*) as well as data for locked retinal derivatives (*8*) are included, then we are able to further constrain the possible solutions. Comparing the distances between carbon atoms C_8-C_{18} calculated for each of the above solutions with rotational resonance ^{13}C NMR data (*12*), and assuming a negative twist for the torsion angle as deduced from studies of locked retinal derivatives (*8*), leads to $\chi_{5,9} = -65°$ for the unique physical solution, i.e., a negatively twisted 6-*s*-*cis* conformation. The above value corresponds to the effective torsional angle of the β-ionone ring relative to the polyene chain and agrees with the refined X-ray structure (*15*). We estimate that the calculated torsion angles are accurate to within $\pm 10°$. The fact that the ^{2}H NMR line shapes are essentially the same to within experimental error over the temperature range from -30 to -150 °C (results not shown) implies that the calculated retinal structure is largely unaffected by chemical exchange, e.g., involving flipping of the β-ionone ring (*15*).

DISCUSSION

Rhodopsin is currently the only G protein-coupled receptor for which the three-dimensional crystal structure is available (*14*−*16*) and consists of the 11-*cis*-retinal prosthetic group bound to the membrane protein opsin (*6*). The mechanism of visual signal transduction initiated by rhodopsin has been extensively investigated (*5*, *42*), in which photolysis of the chromophore gives all-*trans*-retinal, leading to the activated meta II intermediate (*6*). It is known that conformational changes of retinal affect its electronic absorption spectra (*38*) and are crucial for receptor activation (*5*). The nonplanarity of the conjugated retinal polyene chain and the twist of the β-ionone ring are of particular interest (*7*), where the distortion in the vicinity of the 11-*cis* double bond is thought to influence the photoisomerization reaction dynamics (*4*, *7*, *43*). However, the conformations of the polyene chain and β-ionone ring have been rather controversial (*9*, *12*, *15*, *22*), and both 6-*s*-*cis* and 6-*s*-*trans* conformers have been suggested (*9*, *12*, *15*). On the basis of studies of locked retinoids and circular dichroism spectroscopy, it has been concluded that the 6-*s* bond is in a *cis* conformation in rhodopsin (*8*, *13*, *44*). The importance of the β-ionone ring is that its repositioning (*17*) may give receptor activation by helical movements (*6*, *17*, *45*) propagated to the cytoplasmic domains of the protein (*5*, *6*).

In this regard, solid-state ^{2}H NMR spectroscopy can play an important role in providing knowledge of the local

conformation and dynamics of the polyene chain and β-ionone ring of retinal within the binding pocket of rhodopsin. Conformational strain of the retinal ligand is central to current ideas regarding activation of the photoreceptor, and is significant to explaining the quantum yields and mechanism of ultrafast photoisomerization of visual pigments, as well as spectral shifts of the various rhodopsin photointermediates (*46*−*48*). According to the rhodopsin crystal structure (*14*), earlier solid-state ^{13}C NMR studies (*11*), and regeneration data for locked retinoids (*8*, *13*), the β-ionone ring is thought to have a distorted 6-*s*-*cis* conformation. These results agree with density functional theory (DFT) calculations (*25*) and suggest the protein environment contributes to the structural strain of retinal (*7*, *22*, *25*). However, the opposite 6-*s*-*trans* conformation has been proposed on the basis of previous ^2H NMR results (*9*) and quantum mechanical MNDO calculations (*24*). In this case, the minimum energy configuration (*24*) resembles the ^2H NMR structure of the bound retinal (*9*), implying the protein does not appreciably affect the kinetics of the photochemical isomerization (*4*). Although rotational resonance ^{13}C NMR studies (*12*, *18*) now indicate the β-ionone ring has a twisted 6-*s*-*cis* conformation, the issue remains of how to reconcile the ^2H NMR approach with other biophysical methods (*11*, *12*, *14*, *22*, *24*, *25*, *47*).

Solid-State NMR Spectroscopy of Aligned Membrane Samples Containing Rhodopsin. The conclusions of this work involve the application of a new solid-state NMR line shape simulation method developed for the case of a static uniaxial distribution (*20*). At temperatures well below the gel to liquid-crystalline phase transition of the lipid bilayer, rotational and translational diffusion of membrane-bound rhodopsin (*49*) is effectively quenched. As a result, the system can be regarded as a uniaxial distribution of the protein molecules with static rotational disorder on the NMR time scale. One should note that the problem of a static uniaxial distribution with alignment disorder (*30*) is generally relevant to biomembrane constituents in the absence of rotational diffusion (*19*, *50*, *51*), as well as aligned biopolymers including nucleic acids (*52*) and fibrous proteins (*53*). The new line shape distribution function has been applied to investigations of bacteriorhodopsin in aligned purple membranes (*19*, *51*), as well as oriented fibers of DNA (*52*). For the case of aligned membrane specimens one is able to determine the orientations of the isotopically labeled groups relative to the membrane frame. In this way, a set of angular restraints is obtained that can be used for investigations of protein structures in noncrystalline, nativelike bilayer environments.

Besides the orientations of the labeled groups, however, the alignment disorder (mosaic spread) provides a further influence on the solid-state ^2H NMR line shapes. In the case of rhodopsin ($M_r \approx 40$ kDa), the preparation of oriented samples is more challenging than in our earlier studies of the smaller integral membrane protein, bacteriorhodopsin ($M_r = 26$ kDa) (*19*, *51*). Apparently this is due to the presence of substantial cytoplasmic and extracellular domains and the glycosylation of residues Asn^2 and Asn^{15} near the N-terminus (*54*). It follows that the proper treatment of the three-dimensional alignment disorder (mosaic spread) is crucial, particularly when studying the photointermediate states of retinal binding proteins (*51*, *55*). For a static distribution in membrane samples, one must consider the uniaxial distribution of the molecules relative to the local alignment frame *and* the uniaxial distribution of the local frame relative to the average alignment frame, whose principal axis is the average bilayer normal (*20*). The present work shows that reliable bond orientations can be obtained even for mosaic spreads as large as ≈20°. As a result, solid-state NMR of aligned membranes (*19*, *20*, *50*, *56*) can play an important role as an adjunct to X-ray crystallography in investigating the structure and function of membrane proteins (*57*−*59*) as well as other biopolymers (*52*).

Implications of ^2H NMR Results for the Mechanism of Visual Signaling. An important aspect of our findings is that they remove the discrepancy between previous ^2H NMR data (*9*) as compared with solid-state ^{13}C NMR studies (*11*, *12*, *22*) and the X-ray crystal structure (*15*) of rhodopsin. The NMR structure of the retinal chromophore shown in Figure 5 indicates clearly that the ligand is conformationally distorted when bound to the receptor. Current models of torsional strain (*7*, *43*, *60*) of retinal involve steric interactions with rhodopsin as a basis for its ultrafast isomerization kinetics (*7*) and also the energy stored in photolysis (*43*, *61*). The out-of-plane twist of the $C_{12}-C_{13}$ bond is due to a concerted deformation involving the three consecutive bonds from C_{10} to C_{13} and arises from steric hindrance between the C_{13} methyl and the C_{10} hydrogen (*7*, *8*). The importance of the $C_{12}-C_{13}$ bond torsion angle is that photochemical studies suggest it is related to the chemical reaction dynamics (*4*, *7*, *43*). Torsional deformation of retinal is governed by a steep gradient of the excited-state potential energy surface in the Franck−Condon region of vertical excitation, which provides a large driving force for isomerization about the $C_{11}=C_{12}$ bond. The resulting acceleration can account for the ultrafast kinetics of the 11-*cis* to *trans* photoisomerization (*4*) in the visual process. Further nonbonded interactions between the C_8 hydrogen and the C_5 methyl group of the β-ionone ring give torsional twisting about the C_6-C_7 bond (*9*, *12*, *22*), which is formally 6-*s*-*cis* as in the crystal structure of 11-*cis*-retinal (*10*). On the basis of photoaffinity labeling experiments, significant motion of the β-ionone ring has been found in conjunction with the activation of rhodopsin (*17*). In this regard, the potential of ^2H solid-state NMR to reveal dynamical information about the individual methyl groups of retinal within its rhodopsin binding pocket is an important feature of the present method.

As described herein the application of site-directed ^2H NMR spectroscopy provides an important new avenue for investigating photochemical changes of retinal within its rhodopsin binding site in mechanistic detail. By employing a new ^2H NMR line shape treatment (*20*), we obtain a consensus view of the retinal structure in rhodopsin as seen by solid-state NMR spectroscopy, X-ray crystallography, and quantum mechanical calculations. The methods in this article can make significant contributions to elucidating the molecular basis of the inverse agonist and agonist functions of retinal in rhodopsin. These results may also comprise a basis for understanding how interactions of the ligand with rhodopsin are affected by mutations yielding visual diseases such as retinitis pigmentosa.

ACKNOWLEDGMENT

Discussions with R. G. Griffin, M. P. Heyn, and W. L. Hubbell are gratefully acknowledged. We thank R. K. Crouch

for generously supplying protiated 11-*cis*-retinal, T. Huber for help with designing the isopotential centrifugation cells, and S. Krane for assistance with the retinal syntheses.

REFERENCES

1. Mirzadegan, T., Benko, G., Filipek, S., and Palczewski, K. (2003) Sequence analyses of G-protein-coupled receptors: similarities to rhodopsin, *Biochemistry 42*, 2759−2767.
2. Peleg, G., Ghanouni, P., Kobilka, B. K., and Zare, R. N. (2001) Single-molecule spectroscopy of the β_2 adrenergic receptor: observation of conformational substates in a membrane protein, *Proc. Natl. Acad. Sci. U.S.A. 98*, 8469−8474.
3. Alves, I. D., Salamon, Z., Varga, E., Yamamura, H. I., Tollin, G., and Hruby, V. J. (2003) Direct observation of G-protein binding to the human δ-opioid receptor using plasmon-waveguide resonance spectroscopy, *J. Biol. Chem. 278*, 48890−48897.
4. Wang, Q., Schoenlein, R. W., Peteanu, L. A., Mathies, R. A., and Shank, C. V. (1994) Vibrationally coherent photochemistry in the femtosecond primary event of vision, *Science 266*, 422−424.
5. Okada, T., Ernst, O. P., Palczewski, K., and Hofmann, K. P. (2001) Activation of rhodopsin: new insights from structural and biochemical studies, *Trends Biochem. Sci. 26*, 318−324.
6. Hubbell, W. L., Altenbach, C., Hubbell, C. M., and Khorana, H. G. (2003) Rhodopsin structure, dynamics, and activation: a perspective from crystallography, site-directed spin labeling, sulfhydryl reactivity, and disulfide cross-linking, *Adv. Protein Chem. 63*, 243−290.
7. Kochendoerfer, G. G., Verdegem, P. J. E., van der Hoef, I., Lugtenburg, J., and Mathies, R. A. (1996) Retinal analog study of the role of steric interactions in the excited-state isomerization dynamics of rhodopsin, *Biochemistry 35*, 16230−16240.
8. Fujimoto, Y., Fishkin, N., Pescitelli, G., Decatur, J., Berova, N., and Nakanishi, K. (2002) Solution and biologically relevant conformations of enantiomeric 11-*cis*-locked cyclopropyl retinals, *J. Am. Chem. Soc. 124*, 7294−7302.
9. Gröbner, G., Burnett, I. J., Glaubitz, C., Choi, G., Mason, A. J., and Watts, A. (2000) Observations of light-induced structural changes of retinal within rhodopsin, *Nature (London) 405*, 810−813.
10. Gilardi, R. D., Karle, I. L., and Karle, J. (1972) Crystal and molecular structure of 11-*cis*-retinal, *Acta Crystallogr. B28*, 2605−2612.
11. Smith, S. O., Palings, I., Copié, V., Raleigh, D. P., Courtin, J., Pardoen, J. A., Lugtenberg, J., Mathies, R. A., and Griffin, R. G. (1987) Low-temperature solid-state ^{13}C NMR studies of the retinal chromophore in rhodopsin, *Biochemistry 26*, 1606−1611.
12. Spooner, P. J. R., Sharples, J. M., Verhoeven, M. A., Lugtenberg, J., Glaubitz, C., and Watts, A. (2002) Relative orientation between the β-ionone ring and the polyene chain for the chromophore of rhodopsin in native membranes, *Biochemistry 41*, 7549−7555.
13. Fujimoto, Y., Ishihara, J., Maki, S., Fujioka, N., Wang, T., Furuta, T., Fishkin, N., Borhan, B., Berova, N., and Nakanishi, K. (2001) On the bioactive conformation of the rhodopsin chromophore: absolute sense of twist around the 6-*s*-*cis* bond, *Chem. Eur. J. 7*, 4198−4204.
14. Palczewski, K., Kumasaka, T., Hori, T., Behnke, C. A., Motoshima, H., Fox, B. A., Le Trong, I., Teller, D. C., Okada, T., Stenkamp, R. E., Yamamoto, M., and Miyano, M. (2000) Crystal structure of rhodopsin: a G protein-coupled receptor, *Science 289*, 739−745.
15. Teller, D. C., Okada, T., Behnke, C. A., Palczewski, K., and Stenkamp, R. E. (2001) Advances in determination of a high-resolution three-dimensional structure of rhodopsin, a model of G-protein-coupled receptors (GPCRs), *Biochemistry 40*, 7761−7772.
16. Okada, T., Fujiyoshi, Y., Silow, M., Navarro, J., Landau, E. M., and Shichida, Y. (2002) Functional role of internal water molecules in rhodopsin revealed by X-ray crystallography, *Proc. Natl. Acad. Sci. U.S.A. 99*, 5982−5987.
17. Borhan, B., Souto, M. L., Imai, H., Shichida, Y., and Nakanishi, K. (2000) Movement of retinal along the visual transduction path, *Science 288*, 2209−2212.
18. Spooner, P. J. R., Sharples, J. M., Goodall, S. C., Seedorf, H., Verhoeven, M. A., Lugtenburg, J., Bovee-Geurts, P. H. M., DeGrip, W. J., and Watts, A. (2003) Conformational similarities in the β-ionone ring region of the rhodopsin chromophore in its ground state and after photoactivation to the metarhodopsin-I intermediate, *Biochemistry 42*, 13371−13378.
19. Moltke, S., Nevzorov, A. A., Sakai, N., Wallat, I., Job, C., Nakanishi, K., Heyn, M. P., and Brown, M. F. (1998) Chromophore orientation in bacteriorhodopsin determined from the angular dependence of deuterium NMR spectra of oriented purple membranes, *Biochemistry 37*, 11821−11835.
20. Nevzorov, A. A., Moltke, S., Heyn, M. P., and Brown, M. F. (1999) Solid-state NMR line shapes of uniaxially oriented immobile systems, *J. Am. Chem. Soc. 121*, 7636−7643.
21. Feng, X., Verdegem, P. J. E., Edén, M., Sandström, D., Lee, Y. K., Bovee-Geurts, P. H. M., de Grip, W. J., Lugtenburg, J., de Groot, H. J. M., and Levitt, M. H. (2000) Determination of a molecular torsional angle in the metarhodopsin-I photointermediate of rhodopsin by double-quantum solid-state NMR, *J. Biomol. NMR 16*, 1−8.
22. Creemers, A. F. L., Kiihne, S., Bovee-Geurts, P. H. M., DeGrip, W. J., Lugtenburg, J., and de Groot, H. J. M. (2002) ^{1}H and ^{13}C MAS NMR evidence for pronounced ligand-protein interactions involving the ionone ring of the retinylidene chromophore in rhodopsin, *Proc. Natl. Acad. Sci. U.S.A. 99*, 9101−9106.
23. Luca, S., White, J. F., Sohal, A. K., Filippov, D. V., van Boom, J. H., Grisshammer, R., and Baldus, M. (2003) The conformation of neurotensin bound to its G protein-coupled receptor, *Proc. Natl. Acad. Sci. U.S.A. 100*, 10706−10711.
24. Singh, D., Hudson, B. S., Middleton, C., and Birge, R. R. (2001) Conformation and orientation of the retinyl chromophore in rhodopsin: a critical evaluation of recent NMR data on the basis of theoretical calculations results in a minimum energy structure consistent with all experimental data, *Biochemistry 40*, 4201−4204.
25. Sugihara, M., Buss, V., Entel, P., Elstner, M., and Frauenheim, T. (2002) 11-*cis*-retinal protonated Schiff base: influence of the protein environment on the geometry of the rhodopsin chromophore, *Biochemistry 41*, 15259−15266.
26. Borhan, B., Souto, M. L., Um, J. M., Zhou, B., and Nakanishi, K. (1999) Efficient synthesis of 11-*cis*-retinoids, *Chem. Eur. J. 5*, 1172−1175.
27. Botelho, A. V., Gibson, N. J., Wang, Y., Thurmond, R. L., and Brown, M. F. (2002) Conformational energetics of rhodopsin modulated by non-lamellar forming lipids, *Biochemistry 41*, 6354−6368.
28. Gröbner, G., Taylor, A., Williamson, P. T. F., Choi, G., Glaubitz, C., Watts, J. A., deGrip, W. J., and Watts, A. (1997) Macroscopic orientation of natural and model membranes for structural studies, *Anal. Biochem. 254*, 132−138.
29. Levitt, M. H., Suter, D., and Ernst, R. R. (1984) Composite pulse excitation in three-level systems, *J. Chem. Phys. 80*, 3064−3068.
30. Brown, M. F. (1996) Membrane Structure and Dynamics Studied with NMR Spectroscopy, in *Biological Membranes. A Molecular Perspective from Computation and Experiment* (Merz, J., K., and Roux, B., Eds.) pp 175−252, Birkhäuser, Basel.
31. Ulrich, A. S., and Watts, A. (1993) ^{2}H NMR lineshapes of immobilized uniaxially oriented membrane proteins, *Solid State Nuclear Magn. Reson. 2*, 21−36.
32. Siminovitch, D. J., Rance, M., Jeffrey, K. R., and Brown, M. F. (1984) The quadrupolar spectrum of a spin $I=1$ in a lipid bilayer in the presence of paramagnetic ions, *J. Magn. Reson. 58*, 62−75.
33. Gröbner, G., Choi, G., Burnett, I. J., Glaubitz, C., Verdegem, P. J. E., Lugtenberg, J., and Watts, A. (1998) Photoreceptor rhodopsin: structural and conformational study of its chromophore 11-*cis* retinal in oriented membranes by deuterium solid state NMR, *FEBS Lett. 422*, 201−204.
34. Honig, B., Greenberg, A. D., Dinur, U., and Ebrey, T. G. (1976) Visual-pigment spectra: implications of the protonation of the retinal Schiff base, *Biochemistry 15*, 4593−4599.
35. van der Steen, R., Biesheuvel, P. L., Mathies, R. A., and Lugtenburg, J. (1986) Retinal analogues with locked 6−7 conformations show that bacteriorhodopsin requires the 6-*s*-*trans* conformation of the chromophore, *J. Am. Chem. Soc. 108*, 6410−6411.
36. Gibson, N. J., and Brown, M. F. (1993) Lipid headgroup and acyl chain composition modulate the MI-MII equilibrium of rhodopsin in recombinant membranes, *Biochemistry 32*, 2438−2454.
37. Botelho, A. V., Huber, T., and Brown, M. F. (2002) Hydrophobic matching of lipids and rhodopsin in membranes probed by ^{2}H NMR and flash photolysis spectroscopy, *Biophys. J. 82*, 146a.

38. Jäger, S., Lewis, J. W., Zvyaga, T. A., Szundi, I., Sakmar, T. P., and Kliger, D. S. (1997) Chromophore structural changes in rhodopsin from nanoseconds to microseconds following pigment photolysis, *Proc. Natl. Acad. Sci. U.S.A. 94*, 8557−8562.
39. Liebman, P. A. (1962) *In situ* microspectrophotometric studies on pigments of single retinal rods, *Biophys. J. 2*, 161−178.
40. Trouard, T. P., Alam, T. M., and Brown, M. F. (1994) Angular dependence of deuterium spin-lattice relaxation rates of macroscopically oriented dilaurylphosphatidylcholine in the liquid-crystalline state, *J. Chem. Phys. 101*, 5229−5261.
41. Verdegem, P. J. E., Bovee-Geurts, P. H. M., de Grip, W. J., Lugtenburg, J., and de Groot, H. J. M. (1999) Retinylidene ligand structure in bovine rhodopsin, metarhodopsin-I, and 10-methyl-rhodopsin from internuclear distance measurements using ^{13}C-labeling and 1-D rotational resonance MAS NMR, *Biochemistry 38*, 11316−11324.
42. Salamon, Z., Brown, M. F., and Tollin, G. (1999) Plasmon resonance spectroscopy: probing molecular interactions within membranes, *Trends Biochem. Sci. 24*, 213−219.
43. DeLange, F., Bovee-Geurts, P. H. M., VanOostrum, J., Portier, M. D., Verdegem, P. J. E., Lugtenburg, J., and DeGrip, W. J. (1998) An additional methyl group at the 10-position of retinal dramatically slows down the kinetics of the rhodopsin photocascade, *Biochemistry 37*, 1411−1420.
44. Imamoto, Y., Sakai, M., Katsuta, Y., Wada, A., Ito, M., and Shichida, Y. (1996) Structure around C_6-C_7 bond of the chromphore in bathorhodopsin: low-temperature spectroscopy of 6s-*cis*-locked bicyclic rhodopsin analogs, *Biochemistry 35*, 6257−6262.
45. Kim, J. E., Pan, D., and Mathies, R. A. (2003) Picosecond dynamics of G-protein coupled receptor activation in rhodopsin from time-resolved UV resonance Raman spectroscopy, *Biochemistry 42*, 5169−5175.
46. Kochendoerfer, G. D., and Mathies, R. A. (1995) Ultrafast spectroscopy of rhodopsins−photochemistry at its best!, *Isr. J. Chem. 35*, 211−226.
47. Schreiber, M., and Buss, V. (2003) Origin of the bathochromic shift in the early photointermediates of the rhodopsin visual cycle: a CASSCF/CASPT2 study, *Int. J. Quantum Chem. 95*, 882−889.
48. Yan, E. C. Y., Kazmi, M. A., Ganim, Z., Hou, J.-M., Pan, D., Chang, B. S. W., Sakmar, T. P., and Mathies, R. A. (2003) Retinal counterion switch in the photoactivation of the G protein-coupled receptor rhodopsin, *Proc. Natl. Acad. Sci. U.S.A. 100*, 9262−9267.
49. Liebman, P. A., and Entine, G. (1974) Lateral diffusion of visual pigment in photoreceptor disk membranes, *Science 185*, 457−459.
50. Ulrich, A. S., Wallat, I., Heyn, M. P., and Watts, A. (1995) Re-orientation of retinal in the M-photointermediate of bacteriorhodopsin, *Nat. Struct. Biol. 2*, 190−192.
51. Moltke, S. M., Wallat, I., Sakai, N., Nakanishi, K., Brown, M. F., and Heyn, M. P. (1999) The angles beween the C_1-, C_5-, and C_9-methyl bonds of the retinylidene chromophore and the membrane normal increase in the M intermediate of bacteriorhodopsin: direct determination with solid-state ^2H NMR, *Biochemistry 38*, 11762−11772.
52. Nevzorov, A. A., Moltke, S., and Brown, M. F. (1998) Structure of the A-form and B-form of DNA from deuterium NMR line shape simulation, *J. Am. Chem. Soc. 120*, 4798−4805.
53. Yang, Z., Liivak, O., Seidel, A., LaVerde, G., Zax, D. B., and Jelinski, L. W. (2000) Supercontraction and backbone dynamics in spider silk: ^{13}C and ^2H NMR studies, *J. Am. Chem. Soc. 122*, 9019−9025.
54. Huber, T., Botelho, A. V., Beyer, K., and Brown, M. F. (2004) Membrane model for the GPCR prototype rhodopsin: hydrophobic interface and dynamical structure, *Biophys. J. 86*, 2078−2100.
55. Kim, S., Job, C., Wallat, I., Moltke, S., Brown, M. F., and Heyn, M. P. (2001) Retinylidene chromophore orientation in the ground and M-states of bacteriorhodopsin investigated by deuterium NMR spectroscopy, *Biophys. J. 80*, 369a.
56. Marassi, F. M., and Crowell, K. J. (2003) Hydration-optimized oriented phospholipid bilayer samples for solid-state NMR structural studies of membrane proteins, *J. Magn. Reson. 161*, 64−69.
57. Marassi, F. M. (2002) NMR of peptides and proteins in oriented membranes, *Concepts Magn. Reson. 14*, 212−224.
58. Tian, C. L., Tobler, K., Lamb, R. A., Pinto, L. H., and Cross, T. A. (2002) Expression and initial structural insights from solid-state NMR of the M2 proton channel from influenza A virus, *Biochemistry 41*, 11294−11300.
59. Mesleh, M. F., Lee, S., Veglia, G., Thiriot, D. S., Marassi, F. M., and Opella, S. J. (2003) Dipolar waves map the structure and topology of helices in membrane proteins, *J. Am. Chem. Soc. 125*, 8928−8935.
60. Siebert, F. (1995) Application of FTIR spectroscopy to the investigation of dark structures and photoreactions of visual pigments, *Isr. J. Chem. 35*, 309−323.
61. Schick, G. A., Cooper, T. M., Holloway, R. A., Murray, L. P., and Birge, R. R. (1987) Energy storage in the primary photochemical events of rhodopsin and isorhodopsin, *Biochemistry 26*, 2556−2562.

BI0491191